개구부를 갖는 전단벽의 안정해석

Stability Analysis of Concrete Shear Wall System with Opening

이 수 곤* 김 순 철** 송 창 영*** 송 상 용****

Lee, Soo-Gon Kim, Soon-Chul Song, Chang-Young Song, Sang-Yong

Abstract

A concrete shear wall system is commonly adopted in high-rise residential apartment buildings. In the construction stage, a rectangular opening is often made for the convenience of horizontal movement of workers, and construction materials and equipment. In the case of safety or stability assessment of a shear wall, the cutout part can be a critical factor. Finite element method is adopted to investigate the elastic stability behavior of the perforated unit shear wall. The key analysis parameters are the cutout location and its size. The effect of out-of-plane bending and horizontal shear are also examined in the stability analysis.

요 지

철근콘크리트조 고층아파트의 경우 흔히 전단벽식 구조시스템을 채택하게 된다. 이때에는 작업자의 이동과 재료나 장비의 수평 운반 편의상 세대간의 내력벽에 직 4각형 형태의 개구부를 설치할 때가 많다. 이와 같은 개구부는 화재등의 재난시에 신속한 대피용 통로로 이용하도록 하는 경우도 있다. 전단벽의 개구부는 구조체의 안전이나 안정을 위협하는 중요한 요소로 될 수 있으므로 설계시나 안전검토에서 반드시 검토해야할 사항이다. 이번 연구는 개구부를 갖는 직 4각형 전단벽의 탄성안정에 관한 것이다. 연구에서는 유한 요소법을 이용하였고 수치해석의 중요 변수는 개구부의 위치와 크기이다. 또한 연직 하중에 의한 균등 압축응력은 물론 휨 모멘트에 의한 응력 및 수평 전단력이 판의 임계응력에 미치는 영향도 검토하였다. 끝으로 비재하면의 구속이 전단벽의 안정성에 미치는 영향도 검토하였다.

Keywords : Shear Wall, Rectangular Opening, Plane Stress Analysis, Elastic Critical Stress, Finite Element Method, Iteration Method

핵심 용어 : 전단벽, 직 4각형 개구부, 평면 응력해석, 탄성 임계응력, 유한요소법, 반복법

* 전남대학교 건축학부 명예교수
** 동신대학교 건축공학부 교수
*** (주)한국구조물안전원 대표이사
**** 비젼 구조연구소 연구원

E-mail: sgl6323@hotmail.com, 011-607-6323

• 본 논문에 대한 토의를 2005년 12월 31일까지 학회로 보내주시면 2006년 4월호에 토론결과를 게재하겠습니다.

1. Introduction

For the high-rise residential apartment buildings, a concrete shear wall system is commonly adopted. During the construction stage of this shear wall system, a rectangular opening is usually made in the wall (see Fig.1) for easy and rapid movement of construction workers, materials and equipment. The cutout part is usually filled with cement bricks just before the final stage of room finishing. In this case, one can not expect perfect monolithic shear wall behavior especially when it is subjected to wind or earthquake induced horizontal load. This suggests that the perforated part in the shear wall can be a critical factor in the structural design or safety assesement of multi-story shear wall buildings.

Finite element method is adopted to investigate the elastic stability behavior of The perforated unit shear wall shown in Fig. 1. In the wall, cutout location and its size are made to change. The example shear wall has the ratio $a/t = 270cm/18cm = 15 > 10$ and so it is assumed that unit shear wall satisfies Kirchhoff hypothesis.

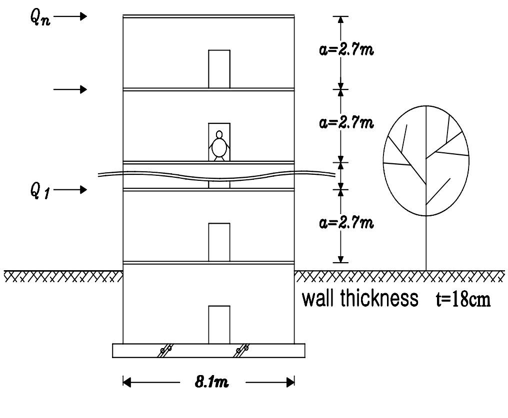

Fig. 1 Schematic view of example shear building

2. Scope of the study

Fig. 2 shows the shear wall unit chosen for the stability analysis by finite element method. In the same figure, two analysis parameters and their change patterns are also shown. As can be seen in the figure, α denotes the maximum flexural to the uniform gravity stress ratio, which is made to change from zero to 0.6 with subinterval 0.2 And β, horizontal shear to gravity force ratio is to change from zero to 0.15 with subinterval 0.05. In the same figure, A, B, C and D designate the locations where the cutout is made. The symbols, C_0, C_1, $\cdots$, C_8 denote the size of the perforated part. For example, C_0 means the wall without opening and C_1 means the wall with an opening of 0.9m (horizontal) × 0.3m (vertical).

Fig. 3 shows the assumed boundary conditions

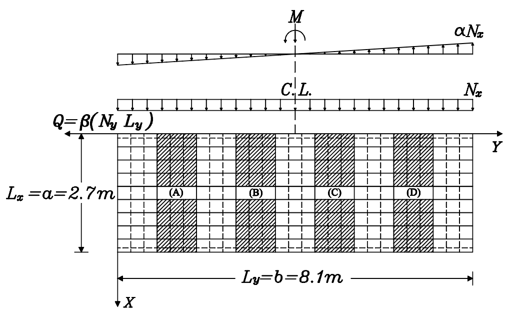

(a) Loading and cutout location (A, B,⋯)

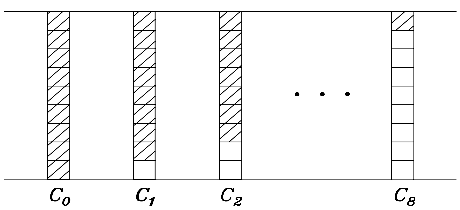

(b) cutout size

Fig. 2 Shear wall unit

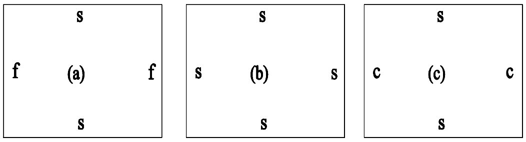

s : simple supported edge,
f : free edge, c : clamped edge

Fig. 3 Boundary conditions

for the shear wall unit. As can be seen in the figure, the loaded edges are simply supported for all of the cases. One can easily expect that the behavior of the plate with the boundary conditions of Fig. 3(a) will be similar to that of a column with simply supported ends. In the shear wall buildings, the deformation of the unloaded edges can be restrained by the columns or by the walls which form right angles to the unloaded edges in the horizontal plan. To take these facts into consideration, unloaded edges are assumed to be either simply supported or completely fixed.

3. Displacement function and element stiffness matrices

3.1 Displacement function

Fig. 4(a) shows a thin rectangular element under the in-plane edge forces and Fig. 4(b) shows three displacement components at a typical node " i ". For 12 degrees of freedom, the element displacement function, w is usually assumed to have the following form

$$w = A_0 + A_1 x + A_2 y + A_3 x^2 + A_4 xy + A_5 y^2 + A_6 x^3 + A_7 x^2 y + A_8 xy^2 + A_9 y^3 + A_{10} x^3 y + A_{11} xy^3 \quad (1)$$

The constants, $A_0, A_1, A_2, \cdots, A_{11}$ can be expressed in terms of nodal displacement components

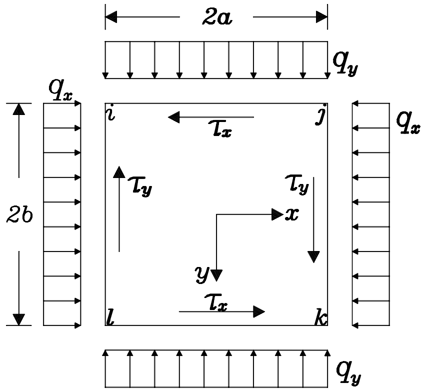

(a) Element under in-plane edge force

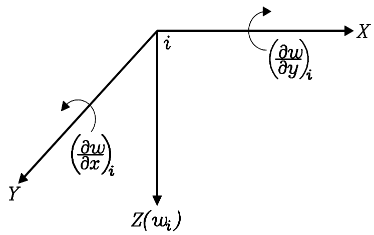

(b) Displacement component

Fig. 4 Rectangular element

and the result leads to

$$w = [f_1, \ f_2, \ \cdots, \ f_{12}] \begin{Bmatrix} \delta_1 \\ \delta_2 \\ \vdots \\ \delta_{12} \end{Bmatrix} = [f]\{\delta\} \quad (2)$$

in which $\{\delta\}$ denotes displacement vector and $[f]$, the shape function set. Shape functions are given by

$$(e = 1/8, \ \varepsilon = x/a, \ \eta = y/b)$$

$$f_1 = e(1-\varepsilon)(1-\eta)(2-\varepsilon^2-\eta^2-\varepsilon-\eta)$$

$$f_2 = e(1-\varepsilon)(1-\eta)(1-\varepsilon^2)a$$

$$f_3 = e(1-\varepsilon)(1-\eta)(1-\eta^2)b$$

$$f_4 = e(1-\varepsilon)(1+\eta)(2-\varepsilon^2-\eta^2-\varepsilon-\eta)$$

$$
\begin{aligned}
f_5 &= e(1-\varepsilon)(1+\eta)(1-\varepsilon^2)a \\
f_6 &= -e(1-\varepsilon)(1+\eta)(1-\eta^2)b \\
f_7 &= e(1+\varepsilon)(1+\eta)(2-\varepsilon^2-\eta^2+\varepsilon+\eta) \\
f_8 &= -e(1+\varepsilon)(1-\eta)(1-\varepsilon^2)a \\
f_9 &= -e(1+\varepsilon)(1+\eta)(1-\eta^2)b \\
f_{10} &= e(1+\varepsilon)(1-\eta)(2-\varepsilon^2-\eta^2+\varepsilon-\eta) \\
f_{11} &= -e(1+\varepsilon)(1-\eta)(1-\varepsilon^2)a \\
f_{12} &= e(1+\varepsilon)(1-\eta)(1-\eta^2)b
\end{aligned}
\qquad (3)
$$

3.2 Element stiffness matrices

The flexural strain energy stored in an element with sides $2a \times 2b$ is given by

$$U = \frac{1}{2}\int_{-b}^{b}\int_{-a}^{a}\{\phi\}^T[D]\{\phi\}dxdy \qquad (4)$$

in which curvature vector, $\{\phi\}$ and elasticity matrix, $[D]$ are given by

$$\{\phi\} = \begin{Bmatrix} \dfrac{\partial^2 w}{\partial x^2} \\ \dfrac{\partial^2 w}{\partial y^2} \\ 2\dfrac{\partial^2 w}{\partial x \partial y} \end{Bmatrix} \qquad (5.a)$$

$$[D] = \frac{Et^3}{12(1-\upsilon^2)}\begin{bmatrix} 1 & \upsilon & 0 \\ \upsilon & 1 & 0 \\ 0 & 0 & 0.5(1-\upsilon) \end{bmatrix} \qquad (5.b)$$

in which ν denotes Poisson's ratio. The external work for the element is given by

$$W = \frac{1}{2}\{\delta\}^T[k]\{\delta\} + \int_{-b}^{b}\int_{-a}^{a}\{\alpha\}^T[N]\{\alpha\}dxdy \qquad (6)$$

in which rotation vector, $\{\alpha\}$ and in-plan force set, $[N]$ are given by

$$\{\phi\} = \begin{Bmatrix} \dfrac{\partial w}{\partial y} \\ \dfrac{\partial w}{\partial x} \end{Bmatrix} \qquad (7.a)$$

$$[N] = \begin{bmatrix} q_x & \tau_x \\ \tau_y & q_y \end{bmatrix} = \begin{bmatrix} q_x & \tau \\ \tau & q_y \end{bmatrix} \qquad (7.b)$$

Equating the strain energy for the element to the external work and using Eq. (2) and (3), one obtains

$$[k] = [k]_b - q[k]_g \qquad (8)$$

Table 1 Flexural stiffness matrix, $[k]_b$

$$
\frac{D}{60ab}
\begin{bmatrix}
60p+60p^{-1}-42-12\mu & & & & & & & & & & & \\
b(60p+6+24\mu) & b^2(80p+16-16\mu) & & & & * \, p=(a/b)^2 & & & symm. & & & \\
a(60p^{-1}+6+24\mu) & 60\mu ab & a^2(80p^{-1}+16-16\mu) & & & & & & & & & \\
30p-60p^{-1}-42+12\mu & b(30p-6-24\mu) & a(-60p^{-1}-6+6\mu) & k_{1,1} & & & & & & & & \\
k_{4,2} & b^2(40p-16+16\mu) & 0 & k_{2,1} & k_{2,2} & & & & & & & \\
-k_{4,3} & -k_{5,3} & a^2(40p^{-1}-4+4\mu) & -k_{3,3} & -k_{3,2} & k_{3,3} & & & & & & \\
30p-30p^{-1}+42-12\mu & b(-30p+6-6\mu) & a(-30p^{-1}+6-6\mu) & k_{10,1} & k_{10,2} & -k_{10,3} & k_{1,1} & & & & & \\
-k_{7,2} & b(20p+4-4\mu) & 0 & k_{11,1} & k_{11,2} & -k_{11,3} & -k_{2,1} & k_{2,2} & & & & \\
-k_{7,3} & k_{8,3} & a^{2(20p}+4-4\mu) & -k_{12,1} & -k_{12,2} & k_{12,3} & -k_{3,1} & k_{3,2} & k_{3,3} & & & \\
-60p+30p^{-1}-42+12\mu & b(-60p-6+6\mu) & a(-30p^{-1}-6+24\mu) & k_{7,1} & k_{7,2} & -k_{7,3} & k_{4,1} & -k_{4,2} & -k_{4,3} & k_{1,1} & & \\
-k_{10,2} & b^2(40p-4+4\mu) & 0 & k_{8,1} & k_{8,2} & -k_{8,3} & -k_{5,1} & k_{5,2} & k_{5,3} & -k_{2,1} & k_{2,2} & \\
-k_{10,3} & -k_{11,3} & a^2(40p^{-1}-16+16\mu) & -k_{9,1} & -k_{9,2} & k_{9,3} & -k_{6,1} & k_{6,2} & k_{6,3} & k_{3,3} & -k_{3,2} & k_{3,3}
\end{bmatrix}
$$

Table 2 Geometric stiffness matrix, $[k]_g$

$$
-\frac{q_x tb}{630a}
\begin{bmatrix}
276 & & & & & & & & & & & \\
66b & 24b^2 & & & & & & & & & & symm. \\
42a & 0 & 112a^2 & & & & & & & & & \\
-276 & -66b & -42a & k_{1,1} & & & & & & & & \\
-66b & -24b^2 & 0 & k_{2,1} & k_{2,2} & & & & & & & \\
42a & 0 & -28a^2 & -k_{3,1} & -k_{3,2} & k_{3,3} & & & & & & \\
-102 & -39b & -21a & k_{10,1} & k_{10,2} & -k_{10,3} & k_{1,1} & & & & & \\
39b & 18b^2 & 0 & k_{11,1} & k_{11,2} & -k_{11,3} & -k_{2,1} & k_{2,2} & & & & \\
21a & 0 & -14a^2 & -k_{12,1} & -k_{12,2} & k_{12,3} & -k_{3,1} & k_{3,2} & k_{3,3} & & & \\
102 & 39b & 21a & k_{7,1} & k_{7,2} & -k_{7,3} & k_{4,1} & -k_{4,2} & -k_{4,3} & k_{1,1} & & \\
-39b & -18b^2 & 0 & k_{8,1} & k_{8,2} & -k_{8,3} & -k_{5,1} & k_{5,2} & k_{5,3} & -k_{2,1} & k_{2,2} & \\
21a & 0 & 56a^2 & -k_{9,1} & -k_{9,2} & k_{9,3} & -k_{6,1} & k_{6,2} & k_{6,3} & k_{3,3} & -k_{3,2} & k_{3,3}
\end{bmatrix}
$$

in which flexural stiffness matrix, $[k]_b$ and geometric stiffness matrix, $q[k]_g$ are given by following tables.

4. Elastic critical load

In the present study, the unit shear wall with sides $2.7m \times 8.1m$ is subdivided into 9×27 square element as shown in Fig. 2. The plane stress analysis of plate under the loading condition together with opening and boundary conditions is performed to determine the in-plane force set, $[N]$ (see Eq. 7.b), which enables one to obtain geometric stiffness matrix for each element.

The structure stiffness matrix for the plate is obtained by combining the element stiffness matrices consecutively. The application of boundary conditions to the assembled matrix leads to

$$([K]_b - \lambda [K]_g)\{\triangle\} = \{0\} \tag{9}$$

where $\triangle$ denotes the nodal displacement vector for the whole plate. The least eigenvalue, or the critical load factor λ_{cr} can be determined by standard eigenvalue iteration technique, for which above equation is transformed into

$$([K]_b^{-1}[K]_g - \frac{1}{\lambda}[I]\{\triangle\} = \{0\} \tag{10}$$

where $[I]$ is the identity matrix.

Some of the critical load coefficients, k de-

Table 3 Critical load coefficients for the plate of Fig.3(a)
$q_{cr} = k \cdot D/b^2$, $(D = Et^3/12(1-\upsilon^2)$, $\upsilon = 0.25)$

$\alpha = 0.0$, *cutout location A*				
	$\beta = 0.0$	$\beta = 0.05$	$\beta = 0.10$	$\beta = 0.15$
C_0	8.84115	8.65017	8.17191	7.53615
⋮	·	·	·	·
C_6	6.90300	6.07464	5.16384	4.41522
C_7	6.68529	5.79654	4.83741	4.07484
C_8	6.41745	5.64246	4.67244	3.86703
$\alpha = 0.2$, *cutout location B*				
	$\beta = 0.0$	$\beta = 0.05$	$\beta = 0.10$	$\beta = 0.15$
C_0	8.35434	7.91613	7.37631	6.81705
⋮	·	·	·	·
C_6	6.68556	6.44202	5.99895	5.46912
C_7	6.47451	6.30666	5.87799	5.32197
C_8	6.25761	6.20460	5.79825	5.20920

Table 4 Critical load coefficients for plate of Fig.3(b)

$q_{cr} = k \cdot D/b^2$, $(D = Et^3/12(1-\upsilon^2)$, $\upsilon = 0.25)$

$\alpha = 0.0$, *cutout location A*				
	$\beta = 0.0$	$\beta = 0.05$	$\beta = 0.10$	$\beta = 0.15$
C_0	11.07954	11.43738	11.80530	12.18177
⋮	·	·	·	·
C_6	9.27837	10.04049	10.70109	11.14524
C_7	8.74260	9.68670	10.51380	11.08404
C_8	8.22654	9.01089	9.78021	10.44909
$\alpha = 0.2$, *cutout location B*				
	$\beta = 0.0$	$\beta = 0.05$	$\beta = 0.10$	$\beta = 0.15$
C_0	10.99692	11.37861	11.77785	12.19428
⋮	·	·	·	·
C_6	8.61597	9.16713	9.74079	10.32543
C_7	8.25066	8.77167	9.29664	9.82269
C_8	7.97967	8.31069	8.59995	8.87355
$\alpha = 0.4$, *cutout location C*				
	$\beta = 0.0$	$\beta = 0.05$	$\beta = 0.10$	$\beta = 0.15$
C_0	10.76841	11.14893	11.54997	11.97270
⋮				
C_6	8.22213	8.68059	9.16110	9.66069
C_7	7.91649	8.39637	8.86869	9.32400
C_8	7.71939	8.22456	8.60859	8.88768
$\alpha = 0.6$, *cutout location D*				
	$\beta = 0.0$	$\beta = 0.05$	$\beta = 0.10$	$\beta = 0.15$
C_0	10.43847	10.79865	11.17827	11.57832
⋮				
C_6	8.18667	8.57214	8.98245	9.41769
C_7	7.87365	8.28468	8.71929	9.17451
C_8	7.58817	8.05023	8.53776	9.03582

termined by repeating above procedures, are listed in Table 3 through 5.

5. Discussion of the results

To date no literature is available to compare the results of the present study except in the cases of plates with C_0 and $\alpha = \beta = 0.0$ (No perforation, no horizontal shear and uniform compression).

Table 5 Critical load coefficients for plate of Fig.3(c)

$q_{cr} = k \cdot D/b^2$, $(D = Et^3/12(1-\upsilon^2)$, $\upsilon = 0.25)$

$\alpha = 0.0$, *cutout location A*				
	$\beta = 0.0$	$\beta = 0.05$	$\beta = 0.10$	$\beta = 0.15$
C_0	11.88261	12.27609	12.69612	13.12686
⋮	·	·	·	·
C_6	9.83421	10.70865	11.52081	12.20292
C_7	9.10656	10.15497	11.12841	11.89116
C_8	8.39349	9.21969	10.05831	10.82493
$\alpha = 0.2$, *cutout location B*				
	$\beta = 0.0$	$\beta = 0.05$	$\beta = 0.10$	$\beta = 0.15$
C_0	11.81358	12.24486	12.69477	13.16223
⋮	·	·	·	·
C_6	9.22329	9.78732	10.37619	10.97946
C_7	8.72388	9.20655	9.70857	10.22634
C_8	8.26515	8.52327	8.78157	9.04329
$\alpha = 0.4$, *cutout location C*				
	$\beta = 0.0$	$\beta = 0.05$	$\beta = 0.10$	$\beta = 0.15$
C_0	11.65680	12.09618	12.55833	13.04379
⋮	·	·	·	·
C_6	8.86302	9.33633	9.82296	10.31967
C_7	8.51769	8.96850	9.39897	9.80946
C_8	8.31042	8.67987	8.94924	9.16164
$\alpha = 0.6$, *cutout location D*				
	$\beta = 0.0$	$\beta = 0.05$	$\beta = 0.10$	$\beta = 0.15$
C_0	11.41776	11.85048	12.30795	12.79098
⋮	·	·	·	·
C_6	8.75700	9.19035	9.64953	10.13310
C_7	8.39259	8.84961	9.32859	9.82251
C_8	8.07768	8.59158	9.12402	9.64692

When the unloaded edges are free, the behavior of the plate with C_0 and $\alpha = \beta = 0.0$ should be similar to that of a column with simply supported ends. In this case, the critical load intensity per unit length of the plate will be given by

$$q_{cr} = k\frac{\pi^2 D}{a^2}, \quad (k = 1.0)$$

From Table 3, one can confirm that the critical load coefficient for the case C_0 and $\alpha=\beta=0.0$ is $k=8.8411/9=0.9823$, which yields the lower bound error, -1.8%. The loading condition for the plate without opening can be represented by Fig. 5 (a). The changes in critical load coefficient are visualized in Fig. 5 (b). It is noticed that the wall (or the column) becomes more unstable as the magnitude of lateral shear force, Q increases.

When the plate edges are simply supported, the stability analysis is somewhat easy. In this case critical load coefficient, k is given

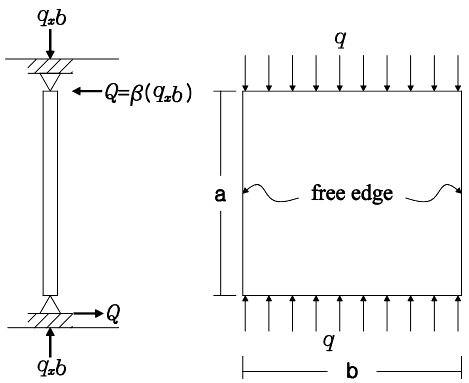

(a) Loading

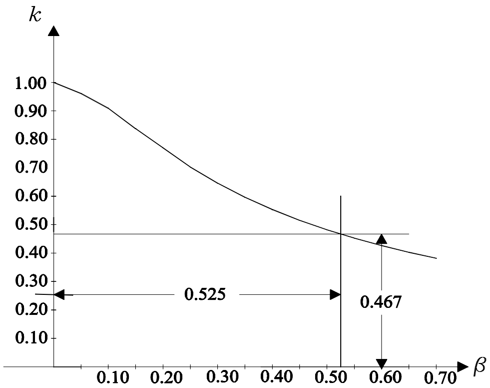

(b) Critical load coefficient

Fig. 5 Fig. 2(a) plate with C_0

$$(a=2.7m,\ b=8.1m,\ m=1)$$

$$k=\left(\frac{mb}{a}+\frac{a}{mb}\right)^2=\frac{100}{9}=11.111$$

The finite element analysis(Table 4) shows critical load coefficient, $k=11.079$, which is 0.28% less than the exact value.

According to Cox's study, the critical load coefficient, k for the plate shown in Fig. 3(a)

$$k=\frac{4}{3}\left[4\left(\frac{a}{b}\right)+\frac{3}{4}\left(\frac{b}{a}\right)^2+2\right]=12.259$$

The finite element analysis(Table 5) is given by $k=11.8826$ resulting in the lower bound error of 3.07%. From the above comparisons of 3 types of plate, one can easily guess the possibility of design aid role of the present study.

Examinations of Table 3 through 5 reveal that critical load coefficient change is decreasing function of cutout size, which can be said the expected results. Also the tables suggest that the cutout part around the unloaded edges is to be avoided when possible. One thing note worthy, in Table 4 and 5, is the increase of horizontal shear force, Q (increase of β) makes the plate more stable, which may be explained with the diagonal tensile force induced by Q.

For easy understanding of plate stability, the changes in the critical load coefficient of Table 4 and 5, that is the coefficients for the boundary conditions of Fig. 3(b) and (c), are visualized in Fig. 6, Fig. 7, Fig. 8 and Fig. 9.

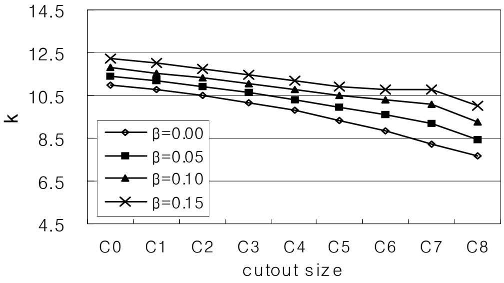

(a) *cutout location A*

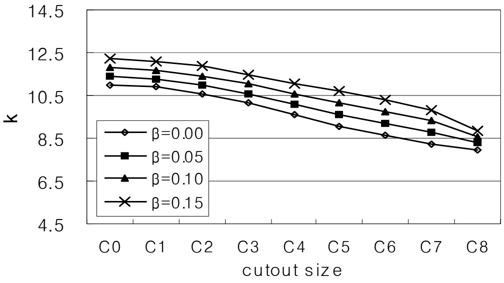

(b) *cutout location B*

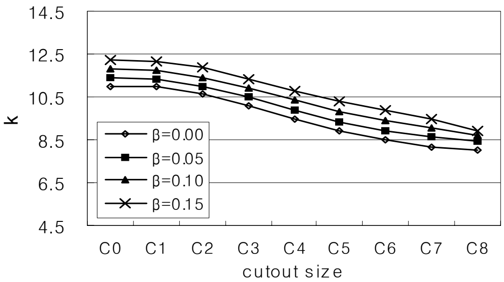

(c) *cutout location C*

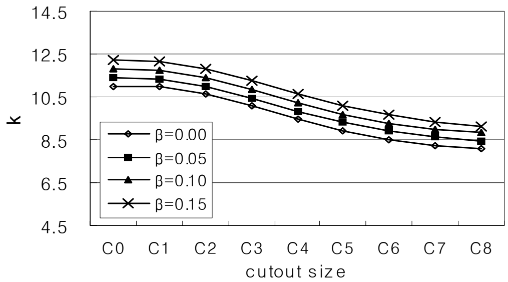

(d) *cutout location D*

Fig. 6 Plate of Fig. 3(b), $\alpha=0.2$

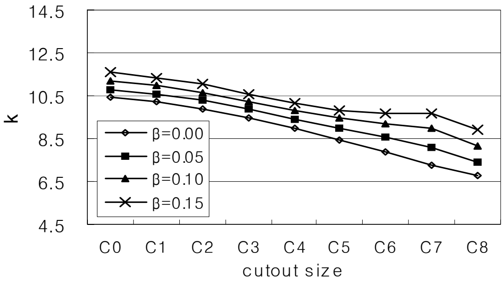

(a) *cutout location A*

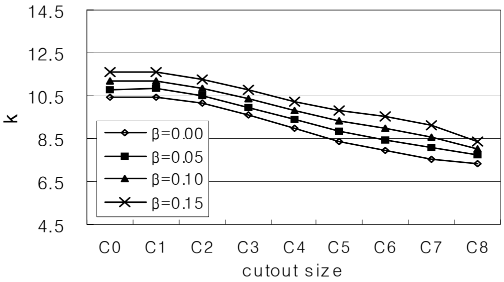

(b) *cutout location B*

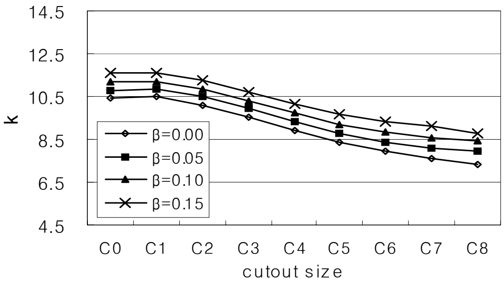

(c) *cutout location C*

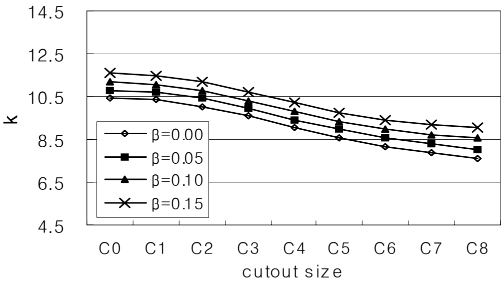

(d) *cutout location D*

Fig. 7 Plate of Fig. 3(b), $\alpha=0.6$

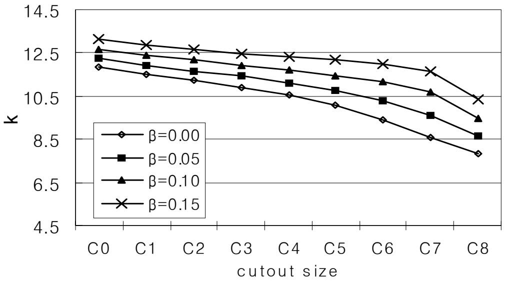

(a) *cutout location A*

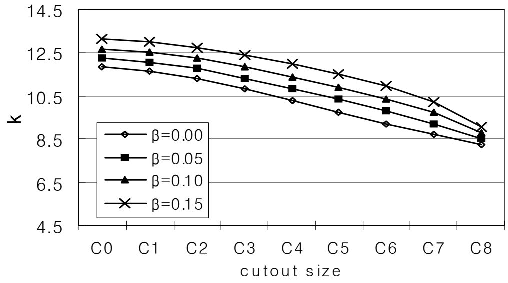

(b) *cutout location B*

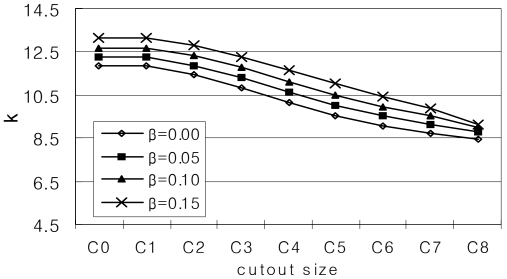

(c) *cutout location C*

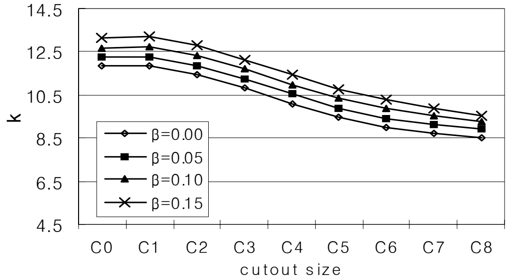

(d) *cutout location D*

Fig. 8 Plate of Fig. 3(c), $\alpha = 0.2$

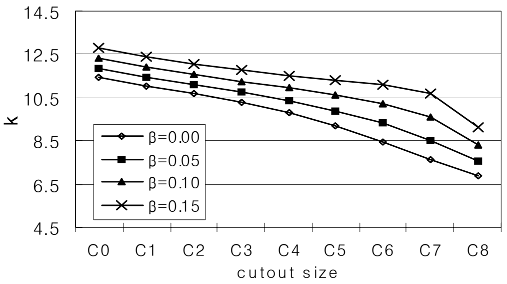

(a) *cutout location A*

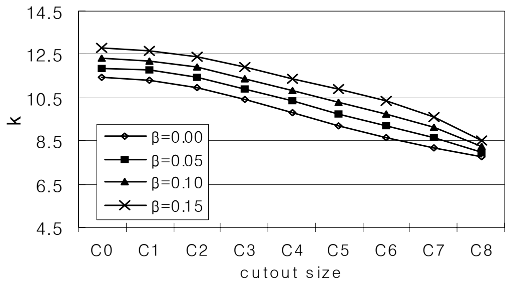

(b) *cutout location B*

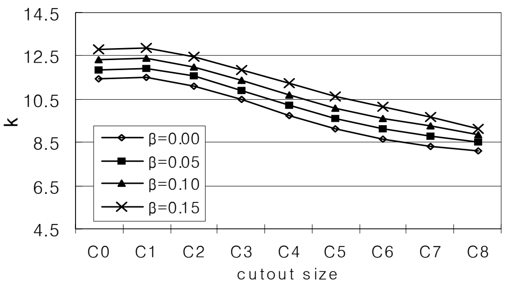

(c) *cutout location C*

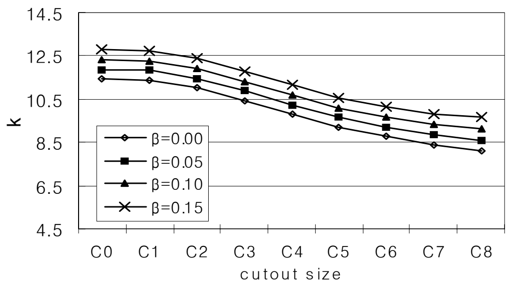

(d) *cutout location D*

Fig. 9 Plate of Fig. 3(c), $\alpha = 0.6$

참고문헌

1. S.G. Lee, S.C. Kim and J.G. Song, "Critical Loads of Square Plate under Different Inplane Load Configurations on Opposite Edges", Journal of Structural Stability and Dynamics, 1(2), 283-291, 2000.
2. N. Yamaki ; Buckling of a Rectangular Plates under Locally Distributed Forces Applied on the Two Opposite Edges, Handbook of Structural Stability, CRC of Japan, 1981.
3. H.L. Lox, The Buckling of Thin Plate in Compress-ion, Handbook of Structural Stability, CRC of Japan, 1981.
4. M.L. Sharp, "Behavior of Plates under Partial Edge Loading", "Proceedings of the sessions related to Steel Structures, Structures Congress '89", San Francisco, 215-224, 1989.
5. M.Z. Khan and K.C. John, "Buckling of Plates under Partial Edge Loadings", J. Struct. Eng, Mech. Div. Proc ASCE EM 5, 67-86, 1962.
6. N. White and W.S. Cottingham, "Stability of Plates under Partial Edge Loadings", J. Struct. Eng, Mech. Div. Proc ASCE EM 5, 67-86, 1962.
7. A. Chajes, "Principle of Structural Stability Theory", Prentice-Hall, Inc., Englewood Cliffs, NJ, 1987.
8. J.S. Kinney, "Indeterminate Structural Analysis", Assison Wesley Publishing Co., Massachusetts, USA, 1975.

(접수일자 : 2005년 6월 2일)